PHYSICAL REVIEW VOLUME 159, NUMBER 2 10 JULY 1967

Superconductive Properties of Ceramic Mixed Titanates

J. F. SCHOOLEY,* H. P. R. FREDERIKSE,† W. R. HOSLER,† AND E. R. PFEIFFER
National Bureau of Standards, Washington, D. C.

(Received 9 December 1966; revised manuscript received 23 March 1967)

The superconducting transition temperatures of a series of mixed barium-strontium and calcium-strontium titanate ceramic specimens have been determined. For several of these samples the low-field magnetization has also been investigated. The results are compared with those obtained from single-crystal $SrTiO_3$.

I. INTRODUCTION

CERAMIC samples of mixed barium-strontium and calcium-strontium titanates have been studied by several methods including x-ray and dielectric-constant measurements.[1–3] The mixed titanates are in general noncubic at low temperatures. Specimens are readily made semiconducting by high-temperature reduction and superconductivity has been observed in these systems.[4]

Because the superconducting transition temperature T_c is an extremely sensitive function of the electron-phonon interaction strength, it appeared reasonable to examine the effect on T_c of the changes in symmetry, lattice constant, and dielectric properties introduced by partial substitution of Ca or Ba into $SrTiO_3$.[5] The transition temperatures of pure $SrTiO_3$ ceramics were compared with those of mixed titanates of the same carrier density n_c. For n_c about $(7\pm4)\times10^{19}$ cm^{-3}, T_c of the mixed titanates was greater by about a factor 2 for low Ba or Ca content. A brief report on this work has appeared previously.[4]

We have now completed measurements of T_c versus n_c for a series of these mixed titanate specimens. In addition, we have made low-field magnetization measurements on five of the specimens. The purpose of this paper is to present these results and to discuss them with respect to those already obtained on single-crystal $SrTiO_3$ specimens.[6,7] We shall find that the particle nature of the ceramic specimens is reflected in the magnetic measurements but not in T_c, and that the changes in the electric properties resulting from addition of Ca or Ba to the $SrTiO_3$ lattice enhance the superconducting region to a surprising degree.

II. EXPERIMENTAL

A. Sample Preparation

The ceramic samples were made from the highest-purity $SrTiO_3$, $BaTiO_3$, and $CaTiO_3$ powders available. Cylinders approximately 2 cm in diameter and 6 mm long were formed in a 15 000 psi press and subsequently sintered at 1600°C for 1h or longer to ensure an average grain size of 20 μ or larger. The pellets were polished and etched, and grain dimensions were measured using a metallographic microscope. The density of the pellets varied with Ba or Ca content and grain size; it ranged from 3.5 to 5 g/cm^3.

The samples were sawed to an appropriate size for magnetic superconductivity and electrical transport measurements ($3\times1\times10$ mm) and made conducting by reduction in H_2 gas at temperatures of 850 to 1350°C for periods of 2 to 27 h. They were cooled to room temperature in flowing He gas as quickly as possible (less than 5 min). The outer surfaces of each specimen were lapped to eliminate any reoxidized layer that might have formed during the cooling period.

B. Hall Measurements

Electron concentrations were derived from the Hall coefficient. Conductivity and Hall measurements were made by standard dc four-probe techniques. Hall contacts were placed at several positions along the length of the sample to check the homogeneity of reduction. Carrier concentration along the length varied less than 10% in any sample, and it remained nearly constant with temperature over the range measured (300 to 1°K). In spite of the rather porous structure generated in promoting large grain size, the room-temperature mobilities were between 50 and 100% of that of single-crystal $SrTiO_3$. The values of n_c appear in Table I.

C. Transition Temperature Measurements

The superconducting transition temperatures of some twenty ceramic specimens were determined by measuring the magnetic susceptibility using the mutual inductance technique. The low-temperature portion of this apparatus is shown in Fig. 1. It consists of a

---

* Supported in part by the Advanced Research Projects Agency.
† Supported in part by the National Aeronautics and Space Administration.

[1] T. Mitsui and W. B. Westphal, Phys. Rev. **124**, 1354 (1961).

[2] E. Hegenbarth, Phys. Status Solidi **9**, 191 (1965).

[3] H. Granicher and O. Jakits, Nuovo Cimento **11**, 480 (1954).

[4] H. P. R. Frederikse, J. F. Schooley, W. R. Thurber, E. Pfeiffer, and W. R. Hosler, Phys. Rev. Letters **16**, 579 (1966).

[5] J. F. Schooley, W. R. Hosler, E. Ambler, J. H. Becker, M. L. Cohen, and C. S. Koonce, Phys. Rev. Letters **14**, 305 (1965).

[6] E. Ambler, J. H. Colwell, W. R. Hosler, and J. F. Schooley, Phys. Rev. **148**, 280 (1966).

[7] J. F. Schooley, W. R. Hosler, E. R. Pfeiffer, M. L. Cohen, and C. S. Koonce (to be published).

TABLE I. Properties of the ceramic specimens.

Specimen	%Ba or Ca	$n_c(10^{19})$	T_c(°K)	H_{c1}(O) (Oe)
43	···	2.7	0.18	
13	···	5.8	0.30	2.8
19	···	6.4	0.25	2.8
27	···	1.7	0.10	
28	···	12.0	0.17	
51	···	23.0	0.10	
14	2.5 (Ba)	6.0	0.52	
37	2.5	0.3	0.23	
15	5.0	6.7	0.50	3.9
16	7.5	7.0	0.29	
31	7.5	0.05	0.22	
33	7.5	34.0	0.09	
35	7.5	0.5	0.25	
48	7.5	2.3	0.27	
53	7.5	15.0	0.45	
6	10.0	4.2	0.25	
17	12.5	4.5	<0.10	
20	2.5 (Ca)	5.0	0.32	
9	5.0	9.2	0.30	
34	7.5	74.0	<0.06	
21	7.5	8.7	0.43	(3.5)[a]
55	7.5	0.2	<0.06	
32	7.5	0.6	0.37	
52	7.5	33.0	<0.07	
36	7.5	2.0	0.48	
56	7.5	0.06[b]	<0.06	
10	10.0	9.3	0.39	
11	20.0	13.0	0.29	
23	30.0	6.7	0.50	1.9
47	30.0	0.6	<0.05	

[a] Specimen CHR21 was not spherical, so that the value of H_{c1}(O) quoted is only approximate.

[b] Hall coefficient appeared to be affected by magnetic history of specimen at liquid helium temperature.

pair of paramagnetic salt cylinders L_1 and L_2 which are composed of powdered manganous ammonium sulfate and powdered potassium chrome alum, respectively, cast with epoxy resin. These cylinders can be cooled by adiabatic demagnetization to respective temperatures of 0.14 and 0.01°K. In turn, L_1 cools a set of electrical leads and the mechanical support M, and L_2 cools a paramagnetic thermometer T and the specimen S, each of which is thermally joined with grease to a bundle of copper cooling wires C which are in turn cast into L_2. After adiabatic demagnetization of L_1 and L_2, a capacitor is discharged through the heater wire H which is wrapped about the specimen. This technique produces a heat pulse which temporarily raises the specimen temperature above T_c, expelling trapped magnetic flux. We compensated stray dc magnetic fields to 0.02 Oe. By using a measuring field of a few milli-oersted, we were able to obtain a superconducting transition nearly free of ac effects as judged by varying the ac field amplitude. The mutual inductance bridge frequency was 270 Hz.

The normal warming of the specimen and cooling salt assembly was quite slow as a result of a stray heat leak of only a few erg/min. For this reason, we ordinarily applied heat through the resistance coil H to obtain curves as shown in Fig. 2, allowing a few minutes for thermal equilibration between readings. It is perhaps worth noting that we used a single-crystal sphere of cerous magnesium nitrate as a thermometer in these measurements. The increased accuracy and reproducibility of this thermometer has enabled us to correct the T_c values of several specimens listed in Table I, Ref. 4. An extended discussion of the calibration of the mutual inductance apparatus appears elsewhere.[7]

The curve of susceptibility versus temperature for specimen CHR43 (Fig. 2) is typical of those obtained for all specimens. The breadth of the transition is much greater than in the single-crystal specimens.[7] We ascribe this result principally to the effect of the superconducting penetration depth λ, which is comparable to the grain size of the ceramic specimens (see Sec. III). The high-temperature tail observed in the transitions in single-crystal specimens[5] usually was present to a greater extent in the ceramic specimens. Very possibly this effect originates in specimen inhomogeneity or in the enhanced specimen surface-to-volume ratios.

Over twenty of these samples have been investigated. The T_c's were determined by fitting the experimental susceptibility data with theoretical curves. The appropriate ratios of λ to grain size a were about unity; in this case the approximate relation $\chi(t)\sim a^2\lambda^{-2}\sim(1-t^4)$ applies. Figure 2 shows a typical example of the fit of a calculated curve to experimental data. The T_c values used in the calculated curves are listed in Table I and are shown in Fig. 3. The extent of the susceptibility tails are indicated by vertical lines in Fig. 3.

D. Magnetization Measurements

The low-field magnetization curves of five of the specimens were measured in a vibrating-coil magnetometer apparatus which has been described previously.[8] The measuring technique used was essentially that followed in the single-crystal studies described in Ref. 6; after adiabatic demagnetization the earth's field compensating coils were adjusted and the specimen

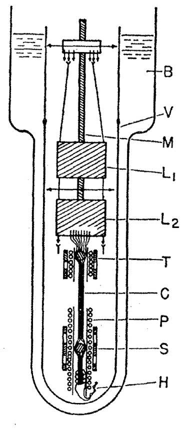

FIG. 1. Schematic drawing of low-temperature portion of mutual inductance apparatus.

---

[8] R. S. Kaeser, E. Ambler, and J. F. Schooley, Rev. Sci. Instr. **37**, 173 (1966).

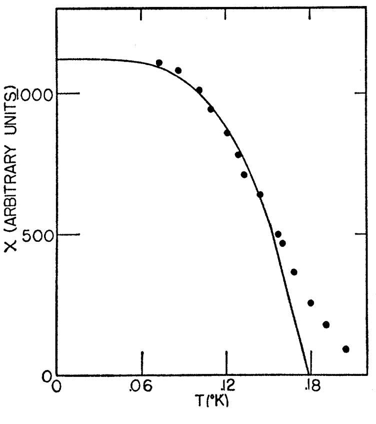

FIG. 2. Susceptibility versus temperature for specimen CHR43 (ceramic $SrTiO_3$). The solid curve is a plot of $\chi=\chi(0)\ (1-t^4)$ fitted preferentially to $|\chi|>0.5|\chi(0)|$.

was driven normal temporarily by means of a heat pulse to expel any trapped flux. After a few minutes equilibration time, the thermometer temperature was measured and the magnetization curve recorded. The heat pulse, equilibration, and thermometer measurement preceded each subsequent magnetization measurement. The magnetization curves taken on specimen CHR13 (pure $SrTiO_3$) are typical of those for all the ceramics, and they are shown in Fig. 4.

We found that the ceramic specimens trap magnetic flux above the lower critical field H_{c1} (Fig. 5). The ratio of trapped flux to peak moment was about 0.5, approximately the same as for the single crystals. Table I shows the extrapolated value of $H_{c1}(T=0)$ deduced from the temperature dependences of $H_{c1}(T)$ for these specimens. We here define H_{c1} as the point at which the magnetization curve first deviates from linearity. As in the single-crystal measurements, this point corresponds to the onset of flux trapping, or hysteresis.[6] This effect can be seen by comparing Figs. 4 and 5.

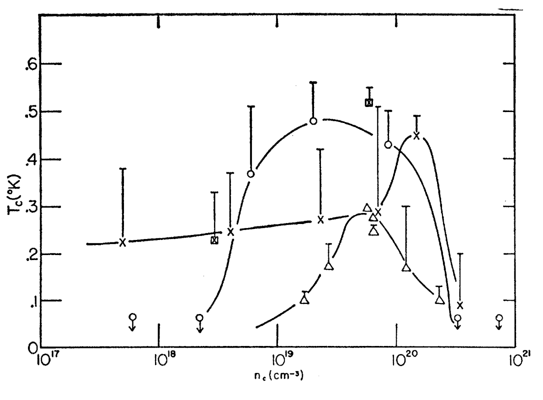

FIG. 3. Superconducting transition temperatures of ceramic samples of (crosses) $Ba_{0.075}Sr_{0.925}TiO_3$, (crosses in squares) $Ba_{0.025}Sr_{0.975}TiO_3$, (circles) $Ca_{0.075}Sr_{0.925}TiO_3$, and (triangles) $SrTiO_3$ of various carrier densities. The vertical lines indicate the extent of the transition breadths beyond the bulk T_c as determined from penetration depth effects.

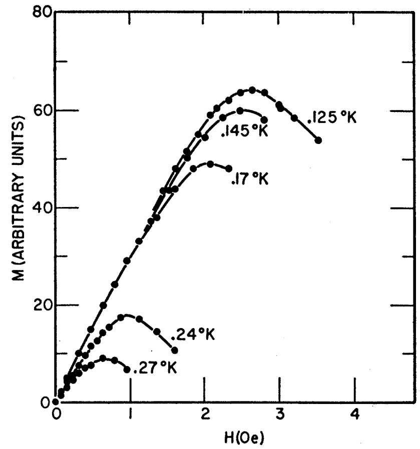

FIG. 4. Low-field magnetization curves at various temperatures for specimen CHR13 (ceramic $SrTiO_3$).

III. DISCUSSION

A. Ceramic $SrTiO_3$

We find that the T_c versus n_c curve for the ceramic $SrTiO_3$ specimens (Fig. 3) is very nearly identical to that obtained for single-crystal specimens.[7] Table I and Fig. 3 reflect data both for mutual inductance and for vibrating-coil magnetometer magnetization experiments. Although T_c appears to be the same for a ceramic as for a single-crystal $SrTiO_3$ specimen, the particulate nature of the ceramic manifests itself in several ways.

First, the initial slope of the magnetization curve (Fig. 4), which is of course the magnetic susceptibility χ, is considerably reduced below that found for a single-crystal specimen (Figs. 2 and 3, Ref. 6). All the specimens involved were shaped into 3-mm-diam spheres, and in each case the position of the vibrating coils was adjusted to maximum sensitivity. Thus the ratio of ceramic to single-crystal susceptibility ≈ 0.5 appears to depend on the particle character of the ceramic specimens. The measured density of the ceramic specimens approaches that of the single-crystal material, but opti-

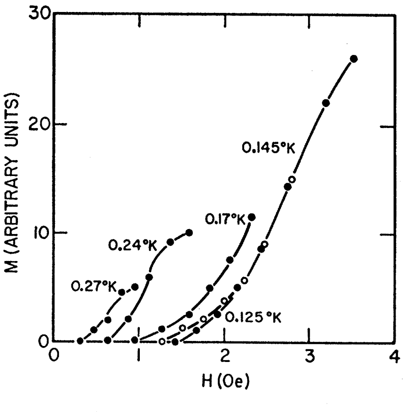

FIG. 5. Trapped flux in specimen CHR13 (same units and temperatures as for Fig. 4).

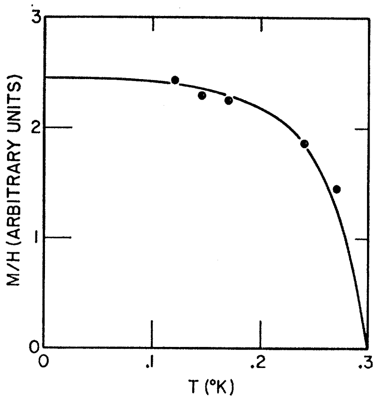

FIG. 6. Magnetic susceptibility of specimen CHR13 versus temperature. Derived from curves of Fig. 4.

cal microscopic examination shows the presence of grains whose size averages 20–40 μ. The penetration depth λ in single-crystal $SrTiO_3$ has been measured, and values in excess of 10 μ have been observed.[9] The reduced values of χ of the ceramic specimens may thus reflect the situation that the applied magnetic field penetrates into the ceramic specimen, presumably along grain boundaries, and that many of the grains appear partially or completely normal because the penetration depth is comparable to the range of the grain dimensions.

A second deviation from the single-crystal results which appears in the measurements on ceramic specimens can again be seen by comparison of Fig. 4 with Figs. 2 and 3, Ref. 6. Whereas the susceptibilities near T_c are indistinguishable from those at low temperatures for the single-crystal specimens (Ref. 6), curves in Fig. 4 corresponding to $T > 0.8T_c$ show a definite decrease in χ. This effect is shown by the points in Fig. 6, which are derived from the curves of Fig. 4. The temperature dependence of χ has been derived for various geometries and λ-to-specimen size ratios.[10] Assuming the relation

$$\lambda(t) = \lambda(0)[1-t^4]^{-1/2},$$

where the reduced temperature $t = T/T_c$, we have drawn a calculated curve for $\lambda(0)/(\text{sphere radius}) = 0.33$ in Fig. 6. This curve fits the experimental susceptibilities reasonably well in spite of the fact that the ceramic specimen is composed of nonspherical grains of a broad range of sizes. This result is further evidence that the magnetic field penetrates the ceramic specimen and that $\lambda(0)$ is comparable to the grain size.

The magnetization curves for specimens CHR15, CHR21, and CHR23, containing 5% Ba, 7.5% Ca, and 30% Ca, respectively, were similar in most respects to those of specimen CHR13.

As we pointed out in Sec. IIC, the mutual inductance transitions are quite broad in the ceramic specimens. We interpret this breadth primarily as illustrating the presence of penetration depth effects, corroborating the results of the magnetization experiments described above. Evidence for this conclusion is that the susceptibility data can be fit reasonably well by curves calculated on the basis of penetration depths of the order of those obtained in single-crystal measurements[9] (see Fig. 2), and that the T_c values so obtained agree with those of the corresponding single-crystal specimens (which exhibit relatively sharp transitions). Thus the "penetration depth" T_c is probably most characteristic of the bulk specimen.

The above arguments do not explain the superconductivity remaining "above T_c" (see Figs. 2 and 3). This effect can be interpreted as resulting from variation in carrier concentration or in chemical composition within the specimens, or from the relatively large surface area of the ceramic particles. Some variation in n_c is to be expected in any semiconductor, and such a variation would be reflected in a variable T_c within the specimens. Thus this effect can be invoked to explain the high-temperature susceptibility tail in all specimens excepting perhaps those lying at a maximum in T_c. However, the lack of pronounced tails in the transitions of the low-T_c specimens CHR 27, 51, 52, and 55 is difficult to account for on this basis. A further difficulty with this explanation is seen in the $Ba_{0.075}Sr_{0.925}TiO_3$ data of Fig. 3; an accounting for the breadth of the transitions observed in the low-n_c specimens would require substantial fractions of the specimens to possess values of n_c greater than the average measured values by factors up to 100 or more, which seems unlikely. Variation in chemical composition within the specimens may contribute to the transition breadths in the mixed titanates, assuming that compositions of higher T_c exist for given values of n_c. Most comments regarding the effect of surfaces on T_c in these materials would be highly speculative; however, the possibility exists that surface reoxidation can occur in reduced semiconductors. This effect probably would result in a lower value of n_c at the surface with a corresponding enhancement in T_c only for specimens of $n_c \gtrsim 10^{20}$ cm^{-3}. A more exhaustive study of specimens of a wide range of composition, carrier concentration, and preparative techniques is probably necessary for an adequate discussion of this problem.

B. Mixed Titanates

In his discussion of the optimum conditions for superconductivity in semiconductors, Cohen[11] places considerable emphasis on the presence of a large number of degenerate valleys, a large density of states, many charge carriers, and a high static dielectric constant.

---

[9] E. R. Pfeiffer and J. F. Schooley, Bull. Am. Phys. Soc. **11**, 209 (1966). A more comprehensive publication of these results is in preparation.

[10] See, for example, Shoenberg, *Superconductivity* (Cambridge University Press, New York, 1962), Appendix II.

[11] M. L. Cohen, Phys. Rev. **134**, A511 (1964). See also Refs. 4 and 7.

There is strong experimental evidence that semiconducting $SrTiO_3$ fits these requirements well.[12] Although the $SrTiO_3$ crystal structure deviates slightly from perfect cubic at low temperatures (c/a becomes 1.00056 at 80°K and approaches 1.0003 at 40°K [13]), the degeneracy of the three (100) ellipsoids is sufficiently maintained to produce the expected magnetoresistance behavior at low[14] and at high[15] magnetic fields.

Addition of Ca or Ba, however, results in an increasingly noncubic crystal structure. For specimens containing 4 and 8% Ca, Mitsui and Westphal report c/a ratios at 110°K of 1.0010 and 1.0024, respectively.[1] We estimate from the phase diagram of $Ba_xSr_{(1-x)}TiO_3$[3] a low-temperature c/a ratio of 1.0008 or higher for $x=0.075$; the appropriate measurement has not been made. Since the mixed crystals are less perfectly cubic than $SrTiO_3$ itself, one would expect, if anything, a *reduction* in T_c.[16]

The significant result presented in this paper is that for electron concentration smaller than 10^{20} cm^{-3}, T_c has been *enhanced*. At higher carrier concentrations T_c decreases rapidly as for the pure $SrTiO_3$; this is understandable because the screening effect from the electron plasma is operative in both cases.[5] For smaller electron densities, however, T_c is raised to such an extent that a sample containing 7.5% Ba is still superconducting for $n_c < 10^{18}$ cm^{-3}. Considering again the list of parameters important for superconductivity, one sees the possibility that the relatively high transition temperatures of the mixed titanates may result from the dielectric properties of the host lattice. Hegenbarth's dielectric-constant measurements (Fig. 3, Ref. 2) show $\epsilon_0(T\approx0)$ to be larger for $Ba_xSr_{(1-x)}TiO_3$ than for $SrTiO_3$ in specimens with Ba concentration less than 6%. The value of $\epsilon_0(T\approx0)$ measured by Mitsui and Westphal for $SrTiO_3$ differs from that of Hegenbarth; however, $\epsilon_0(T\approx0)$ of $SrTiO_3$ does not appear to be enhanced by the addition of Ca. Our own results (Fig. 3) indicate that superconductivity does not persist to as low carrier density for $Ca_{0.075}Sr_{0.925}TiO_3$ as for $Ba_{0.075}Sr_{0.925}TiO_3$. Clearly there is need for further exploration, both experimentally and theoretically, of the interplay between the normal electric properties and the superconductivity in these systems.

The fact that superconductivity is observed in $Ba_xSr_{(1-x)}TiO_3$ for $x\geq0.1$ and in $Ca_ySr_{(1-y)}TiO_3$ for $y\geq0.3$ is particularly interesting in view of the structural changes in these systems. Comparison of the data of Table I with that of Granicher and Jakits (Fig. 9, Ref. 3) indicates that the Ca–Sr system is superconducting in the tetragonal and "pseudocubic" phases and possibly in the rhombohedral phase. Similarly, superconductivity in the Ba–Sr system extends into the region of tetragonal or lower symmetry, according to the phase diagram (Fig. 3 of Smolenskiy and Rozgachev).[17]

The question of the relationship of ferroelectricity to superconductivity is of current interest. Both of the insulating mixed titanate systems show the peaked temperature dependence of ϵ_0 characteristic of ferroelectrics; the Ca–Sr titanates fulfill *all* the requirements for ferroelectricity when the Ca concentration is less than 11%.[1] It is difficult to obtain values of ϵ_0 in the semiconducting materials and hence the influence of the carriers on the lattice dielectric constant is hard to evaluate. However, Stern has pointed out that the electron plasma is capable of interacting only with the longitudinal optical lattice vibrational modes,[18] leaving unaffected any instability in the soft transverse optical mode (which is responsible for the ferroelectric transition).[19] This contention is supported by the observations of Pawley *et al.* on ferroelectricity in the semiconducting SnTe–GeTe system.[20] Thus some evidence exists that several of the superconducting mixed titanates may be ferroelectrics as well.

ACKNOWLEDGMENTS

We would like to acknowledge gratefully the assistance of Harold Johnson of the Crystal Chemistry Section, National Bureau of Standards, who prepared the ceramics used in these experiments, and we also are grateful to Arnold H. Kahn of the Solid State Physics Section, National Bureau of Standards, for many stimulating discussions relative to the work.

---

[12] See Refs. 1, 2, and 3 and the references in H. P. R. Frederikse, W. R. Thurber, and W. R. Hosler, Phys. Rev. **134**, A442 (1964). Also see H. P. R. Frederikse, W. R. Hosler, and W. R. Thurber, J. Phys. Soc. Japan **21**, Suppl. 1966, p. 32. Further evidence for the correctness of Cohen's criteria can be seen in the work on GeTe and SnTe (R. A. Hein *et al.*, Phys. Rev. Letters **12**, 320 (1960); in *Proceedings of the Ninth International Conference on Low Temperature Physics*, edited by J. G. Daunt, D. V. Edwards, F. I. Milford, and M. Yaqub (Plenum Press, Inc., New York, 1965), p. 604; R. C. Miller, *Thermoelectricity*; *Science and Engineering* (Interscience Publishers, Inc., New York, 1961), pp. 434–442.

[13] F. T. Lytle, J. Appl. Phys. **35**, 2212 (1964).

[14] H. P. R. Frederikse, W. R. Hosler, and W. R. Thurber, Phys. Rev. **143**, 648 (1966).

[15] H. P. R. Frederikse, W. R. Thurber, W. R. Hosler, J. Babiskin, and P. Siebenmann, Phys. Rev. **158**, 775 (1967).

[16] In this respect we might mention that $BaTiO_3$ (Ref. 1) shows already at room temperature a c/a ratio of 1.010, indicating a loss of degeneracy among the (100) valleys, and a consequent marked reduction in T_c; in fact, we have been unable to detect superconductivity in $BaTiO_3$ down to $T\approx0.05$°K. Similarly, we have been unable to detect superconductivity in $KTaO_3$; this material remains cubic to 4.2°K, but measurements by S. H. Wemple [Phys. Rev. **137**, A1575 (1965)] indicate that the effective mass m^* is 0.8 m_0. Compared to $SrTiO_3$ ($m^*\approx4m_0$), the density of states at ehe Fermi surface is thus much reduced in $KTaO_3$, and a marked reduction in T: is to be expected.

[17] G. A. Smolenskiy and K. I. Rozgachev, J. Tech. Phys. **24**, 1751 (1954).

[18] F. Stern, Solid State Phys. **15**, 361 (1963).

[19] H. P. R. Frederikse *et al.* (to be published).

[20] G. S. Pawley, W. Cochran, R. A. Cowley, and G. Dolling, Phys. Letters **17**, 753 (1966).